Astronomical and Astrophysical Transactions (*AApTr*), 2012, Vol. 27, Issue 2, pp. 325–334,
ISSN 1055-6796, Photocopying permitted by license only, ©Cambridge Scientific Publishers

Bulges and discs of spiral galaxies: edge-on perspective

N.Ya. Sotnikova*, V.P. Reshetnikov, A.V. Mosenkov

St. Petersburg State University, St. Petersburg 198504, Russia

Received 1 February, 2012

We present a sample of edge-on spiral galaxies both of early and late types. The sample consists of 175 galaxies in the K_s-filter, 169 galaxies in the H-filter and 165 galaxies in the J-filter. Bulge and disc decompositions of each galaxy image, taken from the Two Micron All Sky Survey (2MASS), were performed. We discuss several scaling relations for bulges and discs which indicate a tight link between their formation and evolution. We show that galaxies with bulges fitted by the Sérsic index $n < 2$ (pseudobulges) have quite different distributions of their structural parameters than galaxies with $n \geqslant 2$ bulges (classical bulges). First of all, the distribution of the apparent bulge axis ratio $q_{\rm b}$ for the subsample with $n < 2$ can be attributed to triaxial, nearly prolate bulges, while $n \geqslant 2$ bulges seem to be oblate spheroids with moderate flattening. Secondly, the Photometric Plane of the sample bulges is not flat and has a prominent curvature towards small values of n. Thirdly, despite of the existence of a clear relation between the flattening of stellar discs h/z_0 and the relative mass of a spherical component, the distributions over both parameters are quite different for galaxies possessing bulges and pseudobulges.

Keywords: Galaxies: infrared, photometry; Spiral edge-on galaxies; Fundamental parameters

1 Introduction

In recent decades a number of studies concerning structural properties of galaxies has been performed. The results of decompositions of near face-on disc dominated galaxies as well as of early-type galaxies yielded a lot of correlations between structural parameters of discs and bulges [1–4].

Among all galaxies edge-on ones are of great interest because they provide a unique possibility to obtain information about the vertical structure of a disc and a bulge. The disc scaleheight z_0 together with the disc scalelength h determine the relative thickness of a stellar disc for each galaxy. This ratio as well as the bulge flattening $q_{\rm b}$ (the ratio of isophote semi-axes) may put constraints on the disc and bulge formation processes and their secular evolution.

There are some difficulties in studying edge-on galaxies and obtaining their structural parameters because of the dust extinction. The possible solution is to analyse

*Corresponding author. Email: nsot-astro@mail.ru

Table 1 Morphological types of the sample galaxies and their fractions

Type	Number	Percentages	Type	Number	Percentages
S0, S0-a	41	23.4	Sbc	21	12.0
Sa	11	6.3	Sc	36	20.5
Sab	15	8.6	Scd	4	2.3
Sb	47	26.9	**Total**	**175**	**100**

observations in the NIR passbands where the extinction is drastically reduced. A detailed study of the discs of edge-on galaxies is described in many papers [5–11]. Almost all these papers dealt with bulgeless or late types edge-on galaxies and did not focus on the properties of bulges. Our study is intended to investigate structural parameters of edge-on galaxies both of early and late types and to join analysis of their bulges and discs in the near-infrared bands.

For our purpose we used the 2MASS-selected Flat Galaxy Catalog (2MFGC) [12] as a source of objects and the 2MASS survey [13] as a source of IR image data. We also used the Revised Flat Galaxies Catalog (RFGC) [14] to add late-type galaxies to our sample. Our selection criteria are presented in [15]. The absolute numbers of galaxies of various morphological types (taken from the LEDA) and their percentages are listed in Table 1.

The distances of the galaxies are taken from NASA/IPAC Extragalactic Database (NED) with the Hubble constant $H_0 = 73$ km s^{-1}/Mpc, $\Omega_{\rm matter} = 0.27$, and $\Omega_{\rm vacuum} = 0.73$. To investigate some kinematical and dynamical properties of the sample galaxies we added information about maximum rotation velocity for each galaxy if it was presented in the LEDA database. The sample consists of 175 galaxies in the K_s-filter, 169 galaxies in the H-filter and 165 galaxies in the J-filter. The full list of the sample galaxies with the basic information about them can be found in [15].

According to the $V/V_{\rm max}$ test [17] our full sample is incomplete but the subsample of galaxies with angular radius $r \geqslant 60''$ is complete ($V/V_{\rm max} = 0.49 \pm 0.03$). This subsample consists of 92 galaxies (47 early-type galaxies and 45 late-type galaxies).

2 Two-dimensional bulge/disc decomposition

We used BUDDA (Bulge/Disc Decomposition Analysis) v2.1 code [18] to perform two-dimensional decomposition of galactic images taken from the database of the All-Sky Release Survey Atlas.

The photometric model consists of two major components: a bulge and a disc. The disc is assumed to be axisymmetric, transparent and is represented by an exponential distribution of the luminosity density. It can be described by the face-on central surface brightness $S_{0,\rm d}$ (in mag per arcsec^2), the scalelength h and the 'isothermal' scaleheight z_0.

For the bulge surface brightness profile the Sérsic law is adopted [16]. The main parameters of this profile are: the central effective surface brightness $\mu_{0,\rm b}$ expressed in mag per arcsec^2, the effective radius of the bulge $r_{\rm e,b}$ and the Sérsic index n, defining the shape of the profile. We also assume that the isophotes of bulges are described by

ellipses with the flatness $q_b = b/a$, where b is the semi-minor axis and a is the semi-major axis of an isophote. The Sérsic index of $n = 4$ represents the de Vaucouleurs profile which is very popular to describe the surface brightness distribution of bright elliptical galaxies and of bulges in early-type spirals. The Sérsic index of $n = 1$ represents the exponential profile of bulges in late-type spirals, of galactic discs and of dwarf elliptical galaxies (see e.g. [3, 19–21]).

To check the reliability of our 2D decompositions, we compared our results with the results obtained by other authors. In the K_s-filter, our sample has 30 galaxies in common with the sample in [7] and 14 galaxies that have been investigated in [5]. All mentioned authors used different decomposition procedures but the results of comparison are in good agreement [15].

3 New evidences for different origin of bulges and pseudobulges

Statistical correlations between structural parameters give us a clue for understanding the formation and evolution of spiral galaxies. Here we present several correlations of the main parameters of the galaxies and some new evidences in favour of existence of two quite different populations of bulges in spiral galaxies – classical bulges and pseudobulges.

For edge-on galaxies morphological types are very subjective because the spiral arms are not seen in this case. That is why we distinguish the galaxies in our sample using the Sérsic index n because there is a good correlation between n and the ratio of bulge and disc luminosities B/D that is known to be a key parameter for classifying spiral galaxies on the Hubble sequence [1, 3].

The distributions of the Sérsic indices of galaxies in three passbands are shown in Fig. 1 (the left plot). The distributions demonstrate a weak bimodality which may reflect the existence of two families of bulges: bulges with $n \geqslant 2$ and bulges with $n < 2$. This bimodality is known for some galaxy samples (e.g. [22]) and probably is real for our sample. As was reported earlier (see e.g. [22, 23]) such a bimodality correlates with morphological type of the bulge. The classical bulges have $n \geqslant 2$ and the so-called pseudobulges have $n < 2$. The classical bulges appear to be similar to elliptical galaxies and have similar properties. It is assumed that these systems were built via minor and major merging. The galaxies with the pseudobulges are thought to be formed via disc instabilities and secular evolution and have disc-like apparent flattening.

3.1 The intrinsic shape of bulges

In Fig. 1 (the right plot) we demonstrate the distributions of model bulge axis ratio q_b for edge-on view. In the case of edge-on galaxies this parameter describes directly the bulge flatness and the intrinsic 3D structure of bulges if they are assumed to be oblate spheroids. The median value of this parameter is ~ 0.63, independently of the band. This is in good agreement with [24, 25]. Thus, in general bulges are definitely nonspherical and flattened. However the question about 3D shapes of bulges and their possible triaxiality is still open, despite of the fact that its solution is thought to be crucial for testing different scenarios of galaxy formation.

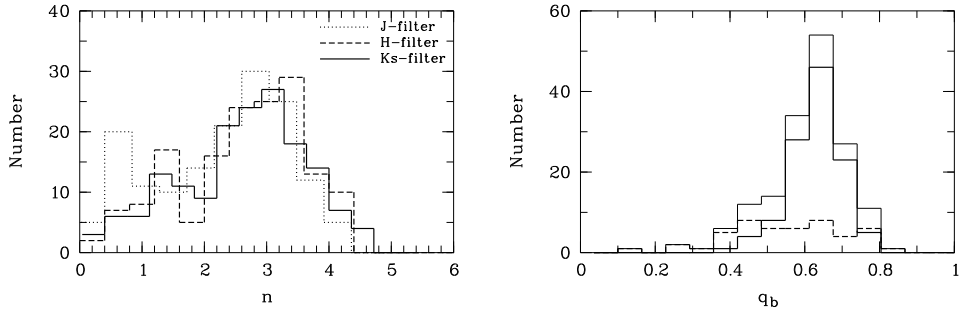


Figure 1 Distributions of the sample galaxies over the Sérsic index of bulges (left) and the model bulge axis ratio q_b in the K_s-band (right). At the right panel the thin line indicates the distribution for the whole sample, the solid line corresponds to the subsample of bulges with $n \geqslant 2$ and the dashed line shows the distribution for the subsample of bulges with $n < 2$.

Our sample of edge-on galaxies allows us to distinguish clearly the difference in the bulge equatorial ellipticities for galaxies with classical bulges and pseudobulges. As one can see in Fig. 1 (the right plot) for classical bulges the distribution of q_b has a rather narrow peak at $q_b \approx 0.65$. This may reflect the fact that the bulges are nearly oblate spheroids with moderate flattening. The distribution of q_b for pseudobulges is very wide, spreading from very flat bulges up to nearly spherical ones. Such a distribution may be attributed to definitely triaxial, near prolate bulges that are seen from different projections – along the major axis and perpendicular to it. But we can not exclude that triaxial shape of bulges in late-type galaxies may hide the presence of bars that thickened in the vertical direction during secular evolution.

Our findings contradict the results obtained in [26]. These authors recovered the PDF (probability distribution factor) for the sample of 148 unbarred S0–Sb galaxies at intermediate inclination angles and concluded that bulges with $n < 2$ show a larger fraction of oblate axisymmetric bulges, a smaller fraction of triaxial bulges, and fewer prolate axisymmetric bulges with respect to bulges with $n \geqslant 2$.

3.2 Photometric plane and Sérsic index

The difference between bulges and pseudobulges arises while building the Photometric Plane for them. This plane represents a tight correlation of the Sérsic index n with the central surface brightness $\mu_{0,b}$ and the effective radius of a bulge $r_{e,b}$ [27, 28]. Performing the least-squared fit of an expression $\log n = a \log r_e + b\,\mu_{0,b} + c$ we obtained a surprising result. It occurred that the galaxies with $\log n \geqslant 0.2$ ($n \geqslant 1.58$) lying on the PhP, that is built for these galaxies, has a small scatter, but the galaxies with $\log n \leqslant 0.1$ ($n \leqslant 1.26$) do not correspond to this plane and form their own plane (Fig. 2). The main difference between our sample and the samples of the above-mentioned works is the range of the shape parameters n. Our sample contains a substantial amount of bulges with $\log n \leqslant 0.1$. For the sample in [27] the low boundary for n lies at $\log n \geqslant 0.2$, that is why the curvature of the Photometric Plane towards small values of n for bulges was not noticed earlier.

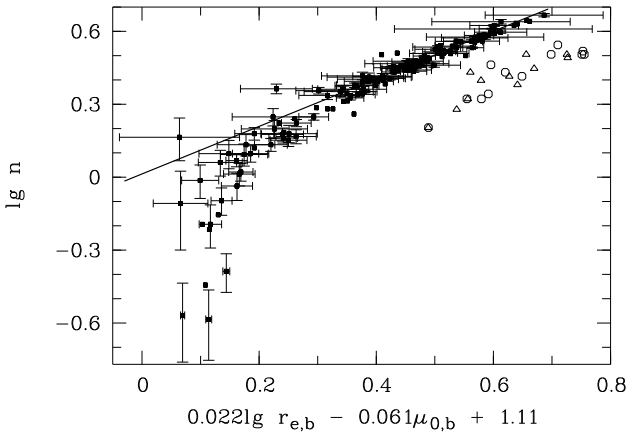


Figure 2 The Photometric Plane built for bulges with $\log n \geqslant 0.2$ of the complete subsample in the K_s-band. The points corresponding to bulges with $\log n \leqslant 0.1$ do not lie in this plane. The model merger remnants of disc galaxies are shown with open circles and triangles [29]. The model data are shifted by a constant along the horizontal axis.

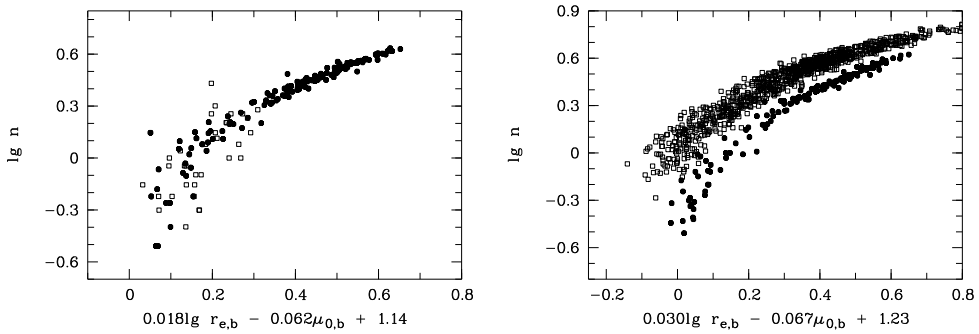


Figure 3 The Photometric Plane built for bulges with $\log n \geqslant 0.2$. Left – the data from [30] (open squares) in comparison with our data (filled circles). Both data are related to the H-band. Right – the data from [31] (open squares, the i-band) in comparison with our data (filled circles, the J-band).

It is not clear whether two distinct parts of the curve in Fig. 2 reflect the different origin of bulges lying in the corresponding regions. However, the collisionless merger remnants of disc galaxies obtained in N-body simulations and fitted by a Sérsic profile fairly well reproduce the slope of the PhP in the region of $\log n \geqslant 0.2$ [29]. We put on the data from [29] in our Fig. 2 and found the numerical data are consistent with our observational ones. The curvature of the PhP towards small values of n may reflect the quite different nature of such bulges, formed, e.g., via secular evolution of discs.

The found curvature is not the feature of our decomposition. It was not noticed earlier because of a lack of substantial number of late-type galaxies in the samples that were studied. We constructed the Photometric Plane based on the samples presented

in [30, 31]. The first sample contains 121 face-on and moderately inclined late-type spirals with derived structural parameters of bulges and discs in the H-band. Figure 3 (the left panel) shows the Photometric Plane for the bulges from [30] together with our data. The plot displays the same feature as Fig. 2: a very tight correlation for classical bulges and a fairy large scatter of points for pseudobulges. Surprisingly, both samples follow the same relation. The sample, presented in [31], consists of around 1000 galaxies with determined photometric parameters in the i-band. The most close passband in our sample is the J-band. We displayed the best fitting relation for our data in Fig. 3 (right panel) and added the point from the sample [31]. There is a shift between two relations which is due to the difference in the passbands. But both samples show a prominent curvature towards small values of n.

3.3 The dark halo and disc flattening

The disc flattening can be measured directly only for edge-on galaxies. It is commonly expressed as the ratio of disc scaleheight z_0 to disc scalelength h. This ratio shows a weak trend with Hubble type [5]. Zasov et al. [10] were the first to found that the disc flattening shows a definite trend with the ratio of dynamical mass $\mathrm{M_{tot}}$ to the disc luminosity provided the dynamical mass is defined as the total mass enclosed within the sphere of a radius that is equal to four disc scalelengths. These authors suggested that discs are marginally stable against the growth of perturbations in their planes and bending perturbations and implied the linear relation between the ratio h/z_0 and the ratio of dynamical mass (or dark halo mass) to disc luminosity. It is valid at least for bulgeless galaxies.

The found correlation means that relatively thinner discs in bulgeless galaxies tend to be embedded in more massive dark haloes. Zasov et al. [10] verified the linear trend, obtained analytically, for two different samples of edge-on bulgeless galaxies with known structural parameters in the R- and K_s-band, using the HI line width W_{50} as a measure of dynamical mass. For our sample, which contains a great many galaxies with massive bulges, we performed the same analysis.

We chose the ratio $\mathrm{M_{tot}/M_d}$ to demonstrate a trend for the disc flattening with the relative mass of a spherical component (Fig. 4). We adopted mass-to-light ratios $f_J = 1.5$, $f_H = 1.0$, and $f_{K_s} = 0.8\,\mathrm{M_\odot}/L_\odot$ [32] to get an estimate of the disc mass $\mathrm{M_d}$. The scatter of points in Fig. 4 is rather large in contrast to the results displayed in [10]. It may be caused by uncertainties in velocities and mass-to-light ratio determinations, decomposition errors and disc relaxation processes, that can thicken a disc just above the threshold for marginal stability. But some of this scatter must be real. Sotnikova & Rodionov [33] concluded that the presence of a compact bulge is enough to suppress the bending instability that leads to the disc thickness increasing. A series of N-body simulations with the same total mass of a spherical component (dark halo + bulge) were performed. The final disc thickness was found to be much smaller in the simulations, where a dense bulge is present, than in the simulations with bulgeless systems. The results of N-body simulations of discs starting from an unstable state were summarized in [34]. The ratio z_0/h versus $(\mathrm{M_h} + \mathrm{M_b})/\mathrm{M_d}$ ($\mathrm{M_h}$ is the halo mass within the sphere of radius $4h$ and $\mathrm{M_b}$ is the bulge mass) was plotted and it was shown that there is a clear scatter in this relation, in spite of the same model mass for a spherical component ($\mathrm{M_h} + \mathrm{M_b}$).

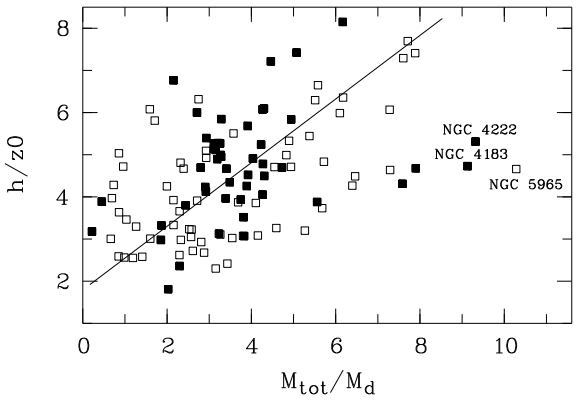


Figure 4 The ratio of h/z_0 as a function of the ratio of dynamical mass to disc mass. The open squares correspond to the subsample of bulges with $n \geqslant 2$, the filled squares refer to the subsample of bulges with $n < 2$. Specially marked points refer to the galaxies with peculiarities in their structure.

Figure 4 shows no difference between galaxies with bulges and pseudobulges but there is a hint of bimodality in the distribution of our sample galaxies over the ratio of the dynamical mass to the stellar mass $M_* = M_d + M_b$ (Fig. 5, the left plot) and over the ratio h/z_0 (Fig. 5, the right plot). This may reflect the presence of two different families of galaxies with different bulges in our sample. Galaxies with pseudobulges possess the large fraction of a dark component and their discs are relatively thinner.

4 Summary and conclusions

We constructed a large sample of edge-on spiral galaxies with performed 2D bulge/disc decomposition of 2MASS galaxies images in J-, H- and K_s-passband using the BUDDA v2.1 package. We extracted global bulge and disc parameters for all objects.

Analysing correlations between structural parameters, including those that describe the vertical structure, we found new evidences in favour of existence of two quite different populations of bulges in spiral galaxies – classical bulges and pseudobulges. Our results can be summarized as follows.

1. The bulge flattening q_b divides the sample into two different families – triaxial, nearly prolate bulges and close to oblate bulges with moderate flattening. The Sérsic index threshold $n \simeq 2$ can be used to identify these two bulge types.
2. The most surprising result arises from the investigation of the Photometric Plane of sample bulges. The bulges with $n \geqslant 2$ populate a narrow strip in their Photometric Plane. However, there is a difference in behavior of this plane for bulges with $n \geqslant 2$ and $n < 2$. The plane is not flat and has a prominent curvature

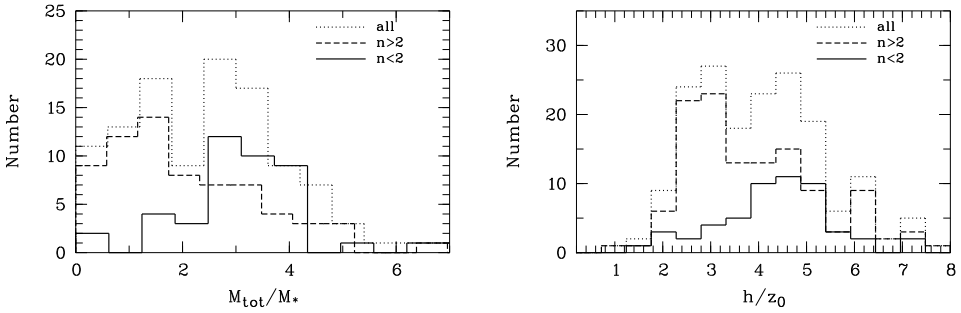


Figure 5 Distributions of the sample galaxies over the ratio of dynamical mass to stellar mass of the galaxy (left) and the ratio of h/z_0 (right). The dotted line indicates the distribution for the whole sample, the dashed line corresponds to the subsample of bulges with $n \geqslant 2$ and the solid line shows the distribution for the subsample of bulges with $n < 2$.

towards small values of n. This result may be due to the physical distinction between classical bulges and pseudobulges.

3. There is a correlation between the relative thickness of stellar discs h/z_0 and the relative mass of a spherical component, including a dark halo. This correlation was known previously for bulgeless galaxies [10] or samples with predominantly bulgeless galaxies [9] and was argued to arise from marginally stable discs. Our sample is much larger than the samples in [9, 10] and more reliable for statistical analysis. Here, we confirm the correlation under discussion. What is more, we do this not for bulgeless galaxies but for galaxies with massive bulges. We conclude that the *total* mass contained in spherical components may be one of the factors that determines the final steady state disc thickness.

Acknowledgments

This work was supported by the Russian Foundation for Basic Research (grant 09-02-00968).

References

[1] R.S. de Jong, Astron. Astrophys. **313** 45 (1996)
[2] C. Möllenhoff, J. Heidt, Astron. Astrophys. **368** 16 (2001)
[3] A.W. Graham, Astron. J. **121** 820 (2001)
[4] S. Courteau, R.S. de Jong and A.H. Broeils, Astrophys. J. **457** 73 (1996)
[5] R. de Grijs, Mon. Not. R. Astron. Soc. **299** 595 (1998)
[6] J.J. Dalcanton and R.A. Bernstein, Astron. J. **124** 1328 (2002)
[7] D. Bizyaev and S. Mitronova, Astron. Astrophys. **389** 795 (2002)
[8] M. Kregel, P.C. van der Kruit and R. de Grijs, Mon. Not. R. Astron. Soc. **334** 646 (2002)

[9] M. Kregel, P.C. van der Kruit and K.C. Freeman, Mon. Not. R. Astron. Soc. **358** 503 (2005)
[10] A.V. Zasov, D.V. Bizyaev, D.I. Makarov and N.V. Tyurina, Astron. Lett., **28** 527 (2002)
[11] D. Bizyaev and S. Mitronova, Astrophys. J. **702** 1567 (2010)
[12] S.N. Mitronova, I.D. Karachentsev, V.E. Karachentseva *et al.*, Bull. Spec Astrophys. Obs., **57** 5 (2003)
[13] M.F. Skrutskie, R.M. Cutri, R. Stiening *et al.*, Astron. J. **131** 1163 (2006)
[14] I.D. Karachentsev, V.E. Karachentseva, Yu.N. Kudrya *et al.*, Bull. Spec. Astrophys. Obs., **47** 185 (1999)
[15] A.V. Mosenkov, N.Ya. Sotnikova and V.P. Reshetnikov, Mon. Not. R. Astron. Soc. **401** 559 (2010)
[16] J.L. Sérsic, Atlas de Galaxias Australes, Observatorio Astronomico, Cordoba (1968)
[17] M. Schmidt, Astrophys. J. **151** 393 (1968)
[18] R.E. de Souza, D.A. Gadotti and S. dos Anjos, Astrophys. J. Suppl. **153** 411 (2004)
[19] G. de Vaucouleurs, Annales d'Astrophysique, **11** 247 (1948)
[20] G. de Vaucouleurs, Mon. Not. R. Astron. Soc. **113** 134 (1953)
[21] K.C. Freeman, Astrophys. J. **160** 811 (1970)
[22] D.B. Fisher and N. Drory, Astrophys. J. **664** 640 (2007)
[23] D.B. Fisher and N. Drory, Astron. J. **136** 773 (2008)
[24] G. Moriondo, C. Giovanardi and L.K. Hunt, Astron. Astrophys. Suppl. **130** 81 (1998)
[25] E. Noordermeer and J.M. van der Hulst, Mon. Not. R. Astron. Soc. **376** 1480 (2007)
[26] J. Méndez-Abreu, E. Simonneau, J.A.L. Aguerri and E.M Corsini, Astron. Astrophys. **521** 71 (2010)
[27] H.G. Khosroshahi, Y. Wadadekar, A. Kembhavi and B. Mobasher, Astrophys. J. **531** L103 (2000)
[28] H.G. Khosroshahi, Y. Wadadekar and A. Kembhavi, Astrophys. J. **533** 162 (2000)
[29] H. Aceves, H. Velázquez, F. Cruz, Mon. Not. R. Astron. Soc. **373** 632 (2006)
[30] L.A. MacArthur, S. Courteau and J.A. Holtzman, Astrophys. J. **582** 689 (2003)
[31] D.A. Gadotti, Mon. Not. R. Astron. Soc. **393** 1531 (2009)
[32] S.S. McGaugh, J.M. Schombert, G.D. Bothun and W.G.L. de Blok, Astrophys. J. **533** L99 (2000)
[33] N.Ya. Sotnikova and S.A. Rodionov, Astr. Lett., **31** 15 (2005)
[34] N.Ya. Sotnikova and S.A. Rodionov, Astr. Lett., **32** 649 (2006)